AAS 08-051

The Evolution of Deep Space Navigation: 1962-1989

Lincoln J. Wood

Jet Propulsion Laboratory, California Institute of Technology

31st ANNUAL AAS GUIDANCE AND CONTROL CONFERENCE

February 1-6, 2008
Breckenridge, Colorado

Sponsored by
Rocky Mountain Section

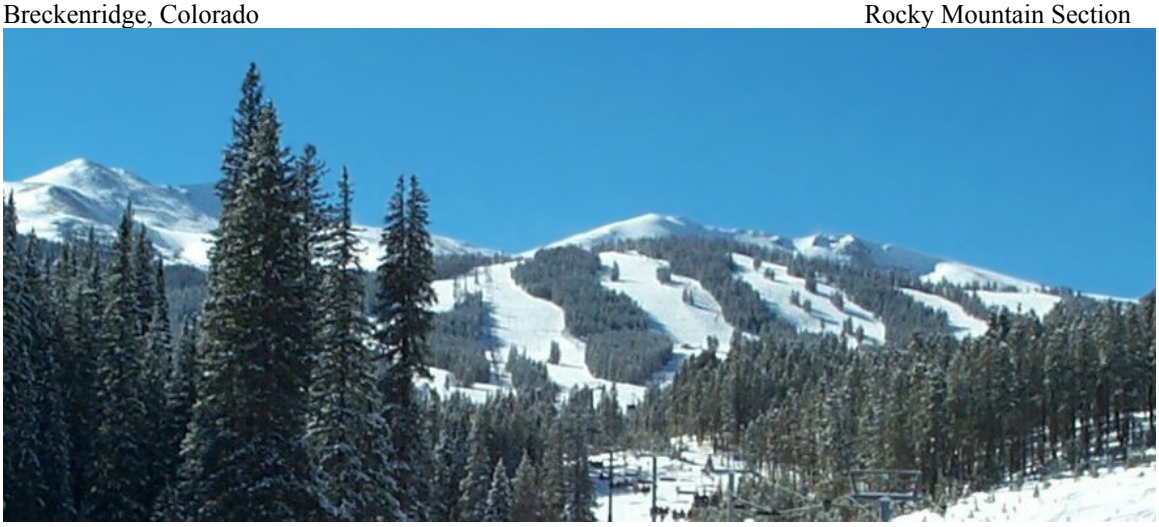

AAS Publications Office, P.O. Box 28130 - San Diego, California 92198

AAS 08-051

THE EVOLUTION OF DEEP SPACE NAVIGATION: 1962-1989

Lincoln J. Wood[†]

The exploration of the planets of the solar system using robotic vehicles began in the early 1960s. Over the years that followed, planetary mission objectives became increasingly sophisticated, as the early single-planet flybys gave way to planetary orbiters, multi-planet flybys, and atmospheric entry and landing missions. During this time the navigational capabilities employed in these missions increased greatly in accuracy, as required by the scientific objectives of the missions and as enabled by improvements in technology.

This paper describes how deep space navigational techniques evolved from the early 1960s through the late 1980s, focusing on both the observational data that were processed to obtain navigational information and the computational techniques that were employed. Radio metric data derived from the spacecraft-to-ground communication link were used throughout this time to yield information about spacecraft position and velocity and other parameters of interest. In order of development and incorporation into use, radio metric data types included Doppler, ranging, and very long baseline interferometric data. The transmission frequencies evolved from L-band, to S-band, to X-band, with substantial reductions in error levels along the way. Optical data, derived from on-board imaging systems, were tested and put into operational use during the 1970s and 1980s, enabling substantial improvements in target-relative navigational accuracies. Computing capabilities and techniques improved substantially during the 1960s, 1970s, and 1980s, allowing problems of greater sophistication to be addressed.

INTRODUCTION

The navigation of a spacecraft is the process of determining the current position and the predicted flight path of the vehicle and correcting the flight path so that it stays within acceptable limits of the desired trajectory. Spacecraft navigation is a complex process involving the collection of data containing information about the position and velocity of the vehicle (and other pertinent quantities as well), followed by the processing of these data to yield estimates of the vehicle's position and velocity as functions of time. Further computation is then needed to plan corrections for the trajectory dispersions away from the desired flight path that inevitably occur. The computational process requires accurate modeling of the motions of the vehicle and the observational data.

A number of robotic spacecraft have traveled throughout the solar system, collecting in-situ and remote scientific observations. In nearly all cases the ability to determine and control the flight path of the vehicle has been critical to mission success.

This paper describes how navigation has been performed for spacecraft designed to travel well in excess of 1,500,000 km from the Earth (such that the gravitational influence of the Earth-moon system is no longer dominant) and that have been targeted to fly close to one or more distant natural bodies. In

[†] Program Manager, Guidance, Navigation, and Control Section, Jet Propulsion Laboratory, California Institute of Technology, Mail Stop 301-150, 4800 Oak Grove Drive, Pasadena, California 91109. Email: Lincoln.J.Wood@jpl.nasa.gov

general, only planetary missions that have been managed by the National Aeronautics and Space Administration (NASA) are discussed. This paper covers the time interval from the launch of NASA's Mariner 2 mission to Venus in 1962 to the Voyager flyby of Neptune in 1989.

NAVIGATIONAL OBJECTIVES IN PLANETARY MISSIONS

All planetary missions involve an approach to at least one celestial body. That body may be simply flown past (or impacted in some fashion), or engines on board the vehicle may be fired to slow it down and place it into orbit around the body. In either case, measurements are acquired as the spacecraft approaches its target; and a spacecraft orbit is determined based on these data. This orbit determination process is repeated as additional measurements are acquired. Trajectory-correction maneuvers (TCMs) are performed several times during the approach, if the predicted encounter conditions are not within some tolerance of the desired conditions. (See Figure 1.) When the last allowable TCM has been performed, typically several days before encounter, the delivery conditions are fixed and cannot be improved further. However, the collection of additional measurements and the generation of subsequent orbit determination solutions allow the trajectory to be predicted more accurately near encounter than it can be controlled. This allows the timing of spacecraft sequences and the pointing of instruments to be adjusted shortly before encounter to optimize the return of scientific data. Measurements that are collected around closest approach are received too late to either modify the encounter conditions or update instrument pointing, but are useful for deducing, after the fact, what the true encounter conditions were, to allow a best reconstructed orbit for science data correlation purposes.

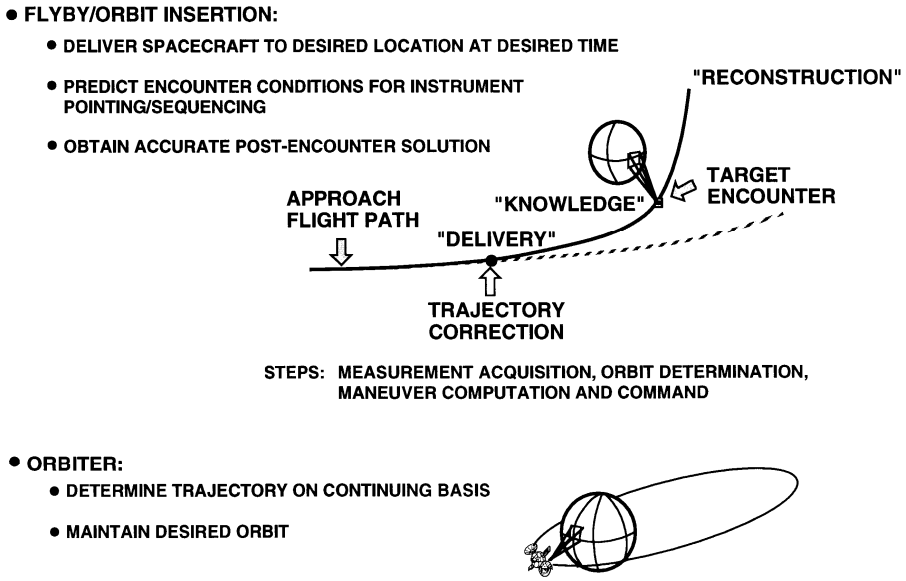

Figure 1 Navigational Objectives in Different Planetary Mission Phases

Many planetary missions involve placing a spacecraft into orbit around some celestial body, rather than flying by, impacting, or gently landing. In this scenario, the orbit of the spacecraft must be determined on a continuing basis, to allow both the correlation of scientific measurements with the locations at which they were recorded and the accurate pointing and sequencing of instruments in the future. In addition, some missions require that the orbit be controlled, so that the spacecraft flies over specific ground features, with specific lighting conditions, etc.

THE DEEP SPACE NAVIGATION SYSTEM

The deep space navigation process can be viewed in the context of a feedback control system, as is shown in Figure 2, with the desired flight path as the principal input and the actual flight path as the principal output. The sections that follow describe the various elements in the feedback control system block diagram, specifically, the spacecraft's orbital dynamics (and the modeling thereof), the various

observational data that may be available for navigational purposes, and the processing of these data to estimate the spacecraft's position and velocity and to compute TCMs.

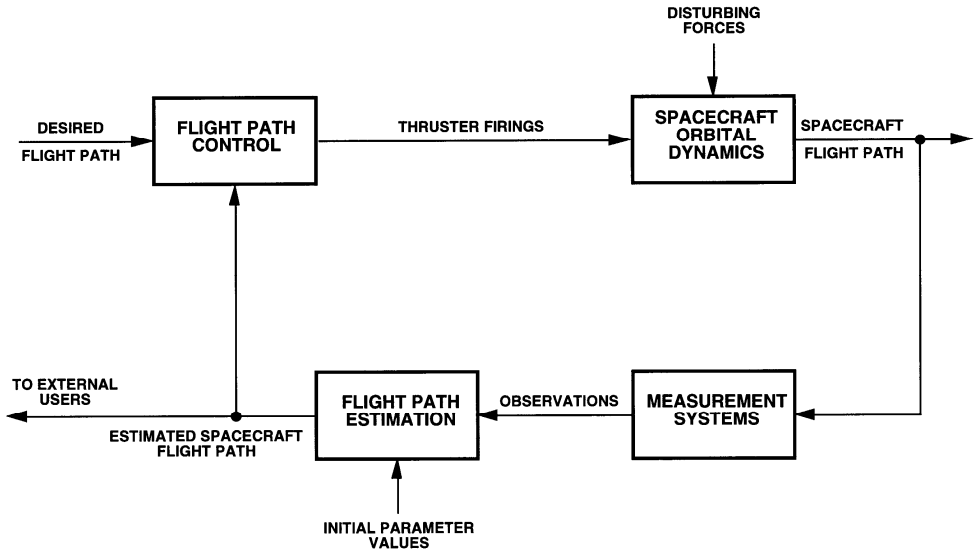

Figure 2 Deep Space Navigation System Block Diagram

Spacecraft Orbital Dynamics and Their Modeling

The acceleration experienced by an orbiting spacecraft can be attributed to a number of effects. The dominant effect is usually gravitational, with one celestial body at a time typically exerting the dominant gravitational influence. The orbital motion of a spacecraft (or a natural body) subject to the influence of a single massive object with a spherically symmetric mass distribution can be described by simple geometric shapes such as ellipses and hyperbolae, as described several centuries ago by Kepler, Newton, and others. Most other forces, gravitational and nongravitational, are small in relative terms and perturb the orbit slightly from these simple geometric shapes. Accurate propagation of spacecraft orbits generally requires numerical integration.

Additional gravitational effects that frequently must be taken into account for the accurate description of spacecraft motion include the gravitational influence of nondominant bodies (such as the Galilean satellites and the sun for a spacecraft orbiting Jupiter), asymmetries in the gravitational field of the dominant body, and general relativistic effects. The terrestrial bodies of the solar system possess inhomogeneous mass distributions; hence, they have complex gravitational fields, which are often described by spherical harmonic expansions. Coefficients in these expansions are often estimated, as part of the navigation process. General relativity causes subtle differences in the motion of a spacecraft and in the propagation of radio signals relative to what would be expected based on classical physics. Deep space measurement systems are sufficiently sensitive to detect some of these small effects.

From time to time, the rocket engines on board a spacecraft must be fired to modify the trajectory of the vehicle. In addition, the motion of a spacecraft is affected by mass expulsion that cannot be precisely modeled or predicted in advance. The attitude of a planetary spacecraft is typically maintained by firing small rocket engines or gas jets. Although these firings are intended to change the orientation of the vehicle, they also change its trajectory. In addition, gas leaks unrelated to commanded attitude control maneuvers can cause deviations in the trajectory. All of these propulsive effects, whether intended or unintended, are often estimated as part of the navigation process.

Spacecraft near atmosphere-bearing bodies are subject to aerodynamic forces. Various parameters in aerodynamic force models can be estimated as part of the navigation process.

Solar radiation pressure exerts a small perturbing influence on interplanetary spacecraft. The resulting acceleration can be modeled, to the extent that the absorptivity and reflectivity properties of the

vehicle are known in advance or can be estimated from navigational data. The reflectivity of spacecraft surface elements can change in flight due to solar wind bombardment.

Early Radio Metric Measurement Systems

The earliest measurements used to navigate planetary spacecraft were derived from the radio link between the spacecraft and the Earth. The Earth-based part of the telecommunication system is a network of large radio telescopes, the Deep Space Network (DSN), three complexes of large radio antennas located near Goldstone, California; Canberra, Australia; and Madrid, Spain. Each complex initially included one or more 26-m antennas, with a single 64-m antenna later added at each complex, beginning in 1966. With the complexes spread between the northern and southern hemispheres and relatively evenly spaced in longitude, any planetary spacecraft can usually be seen from at least one tracking complex at any given time. (In the earliest days of the DSN, it was called the Deep Space Instrumentation Facility (DSIF); the Australian tracking site was not near Canberra; and the tracking site corresponding to the longitude of Europe was located near Johannesburg, South Africa.[1])

The antenna on a planetary spacecraft is able to receive commands transmitted from these ground antennas. The spacecraft antenna, in turn, transmits a phase-modulated signal carrying scientific and engineering data back to one or more ground antennas. For many years, beginning with NASA's first mission to Mars, launched in 1964, planetary spacecraft communicated with the DSN at S-band (2.1 GHz uplink and 2.3 GHz downlink) frequencies.

The earliest radio navigation measurements for planetary missions consisted of Doppler data acquired by the DSN. Electromagnetic radiation transmitted from a ground tracking station to a spacecraft will be received by the spacecraft at a shifted frequency, if the spacecraft and ground station are in relative motion – the so-called Doppler effect. The Doppler frequency shift observed by the spacecraft is proportional to the spacecraft-station relative velocity resolved along the line of sight.

To minimize the effects associated with inconsistencies in ground-based and on-board frequency references, Doppler measurements are generally made in a two-way coherent transmission mode, in which the tracking station continuously transmits and receives. The signal transmitted from the Earth is received by the spacecraft's radio system, which increases its frequency by the multiple 240/221 for S-band links (to avoid interference between the outgoing and incoming signals) and coherently (by means of a phase-locked loop) transmits it back to the Earth. If the distance between the spacecraft and the tracking station is increasing (decreasing), the spacecraft radio system receives and subsequently retransmits a signal whose frequency is shifted to a slightly lower (higher) value by the Doppler effect. On the downlink trip from the spacecraft to the Earth, the frequency of the signal received by the tracking station is again modified by the Doppler effect.

The difference between the frequency received by the tracking station (compensated for the deliberate frequency multiplication in the on-board transponder) and the frequency transmitted at a time corresponding to one round-trip earlier is a measure of the rate of change in the distance between the spacecraft and the tracking station. The integrated difference between the frequency that is received from the spacecraft and the Doppler reference frequency is accumulated as a count of cycles (and fractions thereof) and sampled periodically, yielding a measurement of range change during the count interval.

Doppler data are affected by both random and systematic errors. The random error contributions include receiver noise of various sorts, timing jitter, Doppler counter quantization error, Doppler extractor phase noise, ground equipment path delay phase noise, and frequency standard instability.[2] By the late 1970s, the random error standard deviation for Doppler data with a one-minute count time had been reduced to below 1 mm/s.

In the late 1960s, the capability of measuring spacecraft range was added to the DSN. For most of its history, the DSN has used a binary-coded, sequential-acquisition ranging technique to provide a measurement of the round-trip light travel time between the station and the spacecraft. This travel-time measurement is proportional to the line-of-sight range. An earlier planetary ranging technique used a pseudo-random code. By 1976, ranging instrumentation errors had been reduced to about 20 nanoseconds in round-trip light time, which is equivalent to about 3 m in one-way range.[3]

The ability to make accurate Doppler and range measurements when round-trip signal transit times are fractions of an hour to hours requires very accurate timekeeping. Measurement of spacecraft range to a fraction of a meter requires nanosecond time accuracy at a ground tracking station over the round-trip light time, or clock stability of one part in 10^{13}. Hydrogen masers, as used in the DSN, were stable to 2 parts in 10^{15} over 24 hours, in 1975.[3] This compares to stability of four parts in 10^{12} over one day in 1962 for an early rubidium vapor system.[3]

In the early 1970s, the DSN and some spacecraft were equipped to allow downlink communication at a second, higher frequency of 8.4 GHz in the X-band portion of the microwave region of the electromagnetic spectrum. The downlink transmissions at this frequency were made coherent with the uplink by means of a frequency multiplication in the spacecraft transponder by a factor of 880/221. A number of error sources affecting Doppler and ranging data have lesser impact at X-band than at S-band.

Flight Path Estimation

The position and velocity of a planetary spacecraft are estimated by processing measurements related to some subset of these quantities, in conjunction with very accurate models of the spacecraft dynamics and the measurements. As new measurements, of whatever type, are accumulated, they are compared with the values that these measurements would be expected to have, based on the latest estimates of spacecraft position and velocity and any other quantities that have been selected for estimation. The differences between the actual measurements and their expected values, referred to as measurement residuals, are fed back into the parameter estimation algorithm and used to update the estimates of the parameters in some optimal fashion. This process is illustrated in Figure 3.

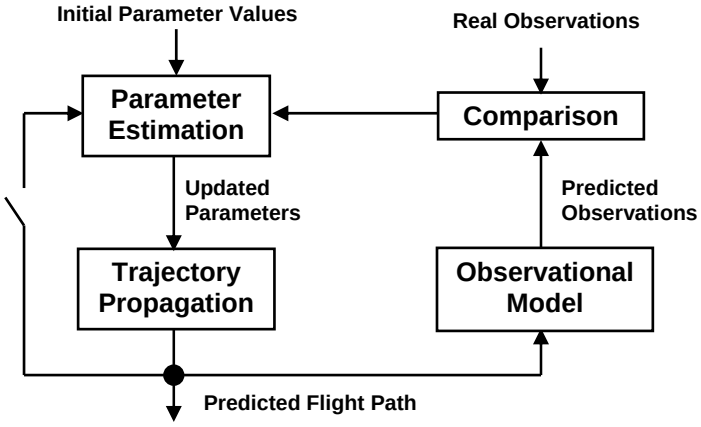

Figure 3 Flight Path Estimation Block Diagram

During the time period covered by this paper, this data processing has always been done in a large ground software system. The Orbit Determination Program (ODP), originally called the Double-Precision Orbit Determination Program, was first delivered for operational use in May of 1969 and was the fundamental software for orbit determination in planetary missions for the next several decades. One of two large modules in this system is the trajectory module, which numerically integrates the trajectory from assumed initial conditions, taking into account all known forces acting on the spacecraft that are large enough to be of consequence. Partial derivatives of the position and velocity components with respect to parameters on which their evolution depends are integrated also. The equations were originally developed in a Cartesian coordinate frame referenced to the Earth's mean equator and equinox of 1950.0. Numerical integration has been performed using a variable-order predictor-corrector method.

A second large module computes simulated observable quantities corresponding to each actual measurement, based on the modeled trajectory, and computes the partial derivatives of the measurements with respect to the initial conditions of the trajectory. It may also compute partial derivatives with respect to a multitude of additional trajectory and observational model parameters, such as those associated with a

planet's gravity field, planetary position coordinates, spacecraft gas leak forces, and tracking-station locations.[4,5]

The estimates of the initial conditions and other parameters are then adjusted until the differences between the actual measurements and the expected measurements, based on the values assumed for the parameters, are minimized in some sense. The estimation algorithm may be a straightforward least-squares procedure, or it may be sequential in time, with stochastic accelerations of the spacecraft modeled as piecewise-constant functions. The estimation process may be performed iteratively until convergence is obtained. The final product of the estimation process is a numerically integrated trajectory that best fits the observations. These computations were carried out exclusively in large mainframe computers for many years. The mainframe computers used include the IBM 7090, IBM 7094, UNIVAC 1108, and UNIVAC 1100/81. During the 1980s the ODP was transported to minicomputers, with the software maintained in both mainframe and minicomputer operating environments to fulfill the desires of various flight projects. The ODP consisted of 300,000 lines of code as of 1979, with FORTRAN V being the primary language.[6]

Random forces, such as thruster firings for attitude control, break the deterministic connection between old and current observations provided by the laws of orbital mechanics. Force mismodeling can produce errors in trajectory estimates that are much larger than the actual trajectory excursions produced by these forces – a reason for the use of sequential estimation including stochastic force models.

The high accuracy required for deep space navigation is achieved with precise observational measurements and precise knowledge of the timing of these measurements, numerically accurate computational algorithms, and a precise modeling of all physical phenomena that affect the values of the observational measurements. Submeter observable modeling is employed throughout the data processing system. Submeter modeling has been achieved by the use of double precision in all trajectory and observable computations, and the use of a relativistic light-time solution algorithm in the Doppler and range observable computations. (Predecessors to the ODP made use of single-precision arithmetic.[7,8]) This algorithm takes into account the retardation in the velocity of light by gravity and the transformation from solar-system barycentric coordinate time to Earth-station proper time.[4]

Physical phenomena that must be modeled accurately include those that affect the values of the measurements directly and those that affect the values of the measurements through their influence on the motion of the spacecraft. Examples of such phenomena include the locations of the tracking stations on the Earth, the Earth's rotational motion, the motions of the Earth, moon, planets, and their natural satellites through the solar system, the gravity-field structures of the massive bodies of the solar system, and the effects of the transmission media on the radio signal. All of these phenomena are modeled in the orbit-determination software. Many require separate, off-line support activities to provide parameter values of the needed accuracy. Descriptions of these support functions are provided in the following subsection.

Navigation Support Functions

Before 1960, planetary ephemerides (tabulated positions as functions of time) relied on astronomical observations of planets and planetary satellites with respect to background stars. This produced errors of several hundred km for the terrestrial planets, assuming perfect knowledge of the Astronomical Unit (AU), essentially the mean distance of the Earth from the sun. The AU is now known to be 149,597,871 km (to the nearest kilometer). Its estimated value, derived from a variety of measurements, was off by 66,000 km as late as 1960, however.[3] A Venus radar experiment, conducted at the Goldstone DSIF facility in early 1961 refined the value of the AU greatly, producing an estimate accurate to ±500 km.[1] This improvement was essential for the planetary missions that were to follow shortly. With the collection of many radar ranging data points to terrestrial planets and information gathered from planetary encounters themselves, as well as additional ground-based optical observations, terrestrial planet ephemeris errors were estimated to be about 0.05 microradians (as viewed from the Earth) in 1982.[2] Ephemeris errors for Jupiter, Saturn, Uranus, and Neptune at that time were estimated to be 10, 20, 40, and 40 times worse.

Position coordinates of the DSN tracking stations in California, Spain, and Australia can be computed in the orbit-determination software from Doppler data taken during previous planetary encounters. A large and expanding data base of planetary-encounter Doppler data was maintained for

many years. As a new planetary ephemeris was generated, or as new encounter data became available, the locations of the Earth tracking stations were recomputed.[9] The locations of DSN tracking stations relative to the Earth's crust had been determined to one-meter accuracy in spin radius and longitude by 1980.[10]

The Earth's spin rate is slowly decreasing and is doing so in an irregular manner, with the length of day varying by several ms over a wide range of time periods.[10] In addition, shifts in the mass distribution of the Earth cause its spin axis orientation to vary with time, with annual variations of about 10 m.[10] These irregularities can be computed by mathematical series expansions, the parameters of which have been determined from centuries of astrometric observations. For many years, universal time and polar motion data were obtained from the Bureau Internationale de l'Heure in Paris, based on its reduction of a large volume of meridian circle and other data. These Earth rotational variations were stored in computer files and applied as calibrations to the computed radio observables. Earth orientation could be predicted one day in advance to one-meter accuracy by 1980.[10]

The refractive effect of the Earth's troposphere results in roughly 2 m of signal path delay at zenith and 20 m at a 6-deg elevation above the horizon.[10] The tropospheric delay can be expressed as the sum of contributions from the wet and dry components of the atmosphere. The dry component contributes about 95% of the total zenith delay, is proportional to the surface atmospheric pressure, and is relatively easy to estimate. The wet component is proportional to the water vapor density along the signal path and is highly unstable. Tropospheric modeling in 1980 was accurate to 4.5 cm for zenith biases and 1 cm for line-of-sight fluctuations over a 10-minute interval at a 15-deg elevation angle.[10]

A radio signal passing through a plasma medium, such as the Earth's ionosphere or interplanetary space, particularly near the sun, experiences an increase in phase velocity and a comparable decrease in group velocity. The cumulative effects on the signal are proportional to the integral of electron density along the signal path. The ionospheric delay varies both diurnally and seasonally. The magnitude of the ionospheric effect at S-band is approximately 3-8 m at zenith during the daytime and an order of magnitude less at night. Solar plasma-induced delays at S-band can range from 10-1000 m, depending on the proximity of the signal path to the sun and the level of solar activity, with drifts of typically about 15 m over an eight-hour tracking pass at a sun-Earth-probe angle of 20 degrees.[10]

For a number of years, charged-particle effects due to the Earth's ionosphere were calibrated by measuring the Faraday rotation of linearly polarized signals transmitted by certain satellites in geostationary orbit.[2] Since a plasma medium has equal and opposite effects on phase and group velocities at the frequencies of interest, and since Doppler data measure phase, while range codes propagate at the group velocity, a comparison of Doppler and ranging data can yield information about the total electron content along the signal path. A computed data type known as DRVID (Differenced Range Versus Integrated Doppler) was developed for this purpose.[10] The effects of charged particles along a signal path can also be calibrated by analyzing the difference in the effects on downlink Doppler data received at two frequencies, assuming that both S- and X-band downlinks are available. X-band radio metric data are much less affected (in the ratio $(3/11)^2$) by plasma interactions than S-band data because of the inverse-square frequency dependence of these interactions.

Trajectory-Correction Maneuvers

The best estimate of the spacecraft trajectory, derived from navigational data, serves as the basis for computation of the velocity-correction parameters. Computation of these parameters is performed in another software module, often taking into account an evolving redesign of the remainder of the mission. The effects of all maneuvers on the future flight path, the science viewing geometries that result, and the predicted propellant expenditure are verified by simulation studies before a maneuver is executed.

A number of propulsive maneuvers are typically required to navigate a deep space mission. Launch injection errors are usually corrected in the first month of travel. Trajectory biases imposed due to planetary quarantine considerations may be eliminated or reduced at the same time. During the transit from Earth to a distant body, a deep-space maneuver may be needed to arrive at the body in a fuel-efficient manner. As the spacecraft approaches the body, one or two maneuvers are required to guide the spacecraft to the desired encounter geometry. If the spacecraft is to orbit the body, a large retro-maneuver is usually

required near the point of closest approach. Subsequent orbit maintenance is usually required throughout the useful lifetime of a planetary orbiter.

The timing of TCMs is governed by the desire to control the trajectory as accurately as possible, while minimizing the expenditure of propellant. Precise determination of the orbit of the spacecraft is essential prior to the computation of each maneuver.

Conceptual Representation of the Deep Space Navigation System

The navigation system that has been used to perform NASA's robotic planetary missions includes the DSN, certain elements of the spacecraft, ground-based computational facilities and software, and various support functions. Figure 4 illustrates the elements of measurement, communication, computation, and propulsion that comprise the overall navigation system that has been employed for NASA's deep space missions. The right side of the diagram shows a spacecraft receiving commands from a ground station and transmitting data to the station. Radio metric data are extracted from the incoming radio signal at the tracking station. Also shown on the right is the capability for spacecraft propulsion. The left side of the diagram depicts the ground processing system used to compute the spacecraft orbit and trajectory-correction parameters.[11]

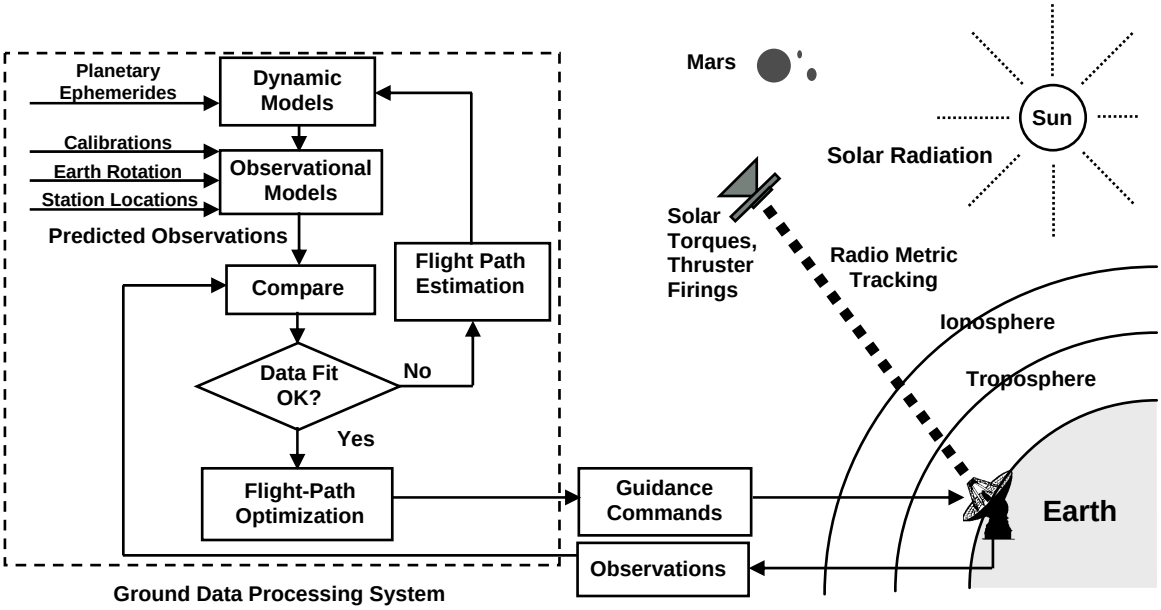

Figure 4 Conceptual Representation of Deep Space Navigation System

NAVIGATIONAL ACCURACY USING DOPPLER AND RANGING DATA

Navigational accuracy for interplanetary flight can be characterized by the uncertainty with which a spacecraft is delivered to its target. The delivery error to a planet or distant satellite is usually dominated by the target-relative orbit determination error. Maneuvers are typically performed shortly before target encounters, and position errors due to both maneuver magnitude and direction errors normally do not have time to increase appreciably before the encounter is achieved.

For a distant spacecraft, the station-relative range rate is approximately equal to the geocentric range rate plus a sinusoidally varying term associated with the Earth's rotation. (See Figures 5 and 6.) The phase of the sinusoidal signal is linearly related to the right ascension of the spacecraft (the angle from the vernal equinox direction to the projection of the spacecraft's position vector onto the Earth's equatorial plane), and the amplitude is proportional to the cosine of the spacecraft's geocentric declination (the angle between the spacecraft's position vector and the equatorial plane).[12]

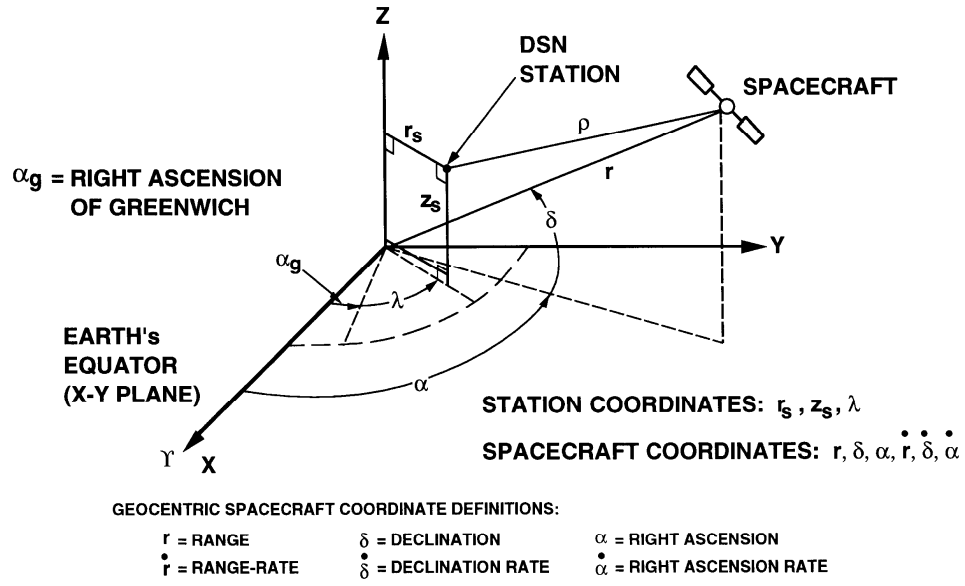

- SPACECRAFT TRAJECTORY IS DESCRIBED BY 6-PARAMETER STATE VECTOR OF POSITION AND VELOCITY COMPONENTS

Figure 5 Basic Elements of Spacecraft Trajectory Information

- TWO-WAY RANGE AND DOPPLER DIRECTLY MEASURE LINE-OF-SIGHT COMPONENTS OF SPACECRAFT STATE
- DIURNAL SIGNATURE OF EARTH ROTATION ALSO PROVIDES ANGULAR STATE INFORMATION

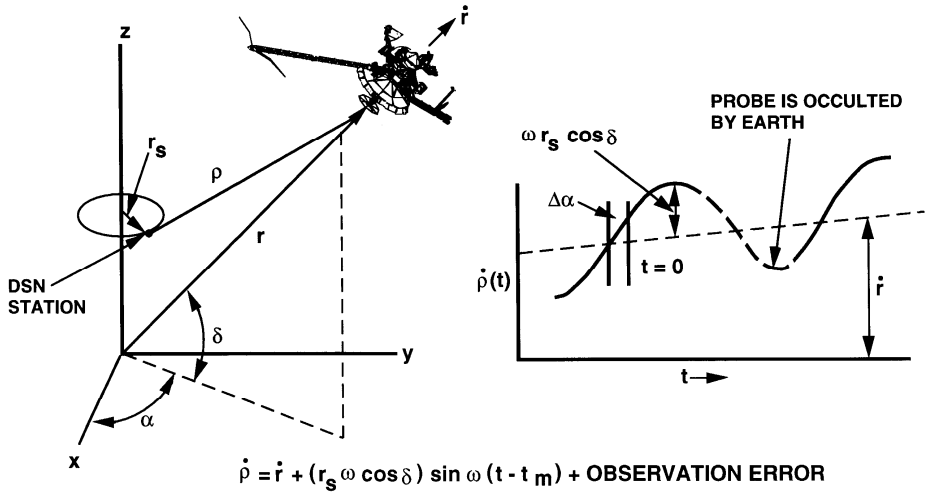

Figure 6 Range and Doppler Tracking

Thus, a time series of Doppler data can be used to infer the direction to the spacecraft, in terms of its right ascension and the cosine of its declination. The sensitivity of the Doppler data to the declination is proportional to the sine of the declination, which causes a degradation in orbit determination accuracy at declinations near zero. The accuracy of the determination of right ascension is not particularly sensitive to variations in geometry. An obvious concern therefore develops if a target planet is near zero declination when encountered by a spacecraft. In the context of the simple model described above, a singularity

occurs, and the Doppler-based orbit determination uncertainties in declination increase sharply. Fortunately, declination usually changes fairly rapidly in flights to the terrestrial planets, so that the singular condition does not exist for long. For declinations not close to zero, two days of Doppler tracking would typically yield a spacecraft angular position determination relative to the Earth accurate to a few tenths of a microradian by 1976.[3] The third spacecraft position component could be determined quickly by measuring range.

Now let us consider a situation in which the spacecraft velocity components are relatively poorly known, perhaps because the spacecraft has just performed a propulsive maneuver. Such maneuvers are always subject to errors in execution,[13] so that the achieved spacecraft velocity will not exactly match the intended value. The radial velocity component can be determined immediately, to the accuracy of the Doppler data. The perpendicular velocity component in the direction of the spacecraft's apparent motion across the celestial sphere is the next easiest to determine. The orbital motion of the spacecraft in the sun's gravitational field dictates a relationship between this velocity component and the time rate of change of the line-of-sight component. Thus, by observing the rate of change of the line-of-sight velocity, this second velocity component can be determined. It was estimated in 1976 that this velocity component could typically be determined to perhaps 10 mm/s with several hours of Doppler tracking data, with further accuracy improvement available after several days of tracking.[3] The third velocity component, perpendicular to both the line of sight and the spacecraft's motion across the celestial sphere, becomes well determined only after a few weeks of tracking.[3]

This discussion applies to the cruise and distant approach phases of planetary missions. Once a spacecraft is well within the gravitational field of a distant body, whether flying by or as a captured satellite, its orbit can be computed more accurately from Doppler data than it can be computed during the cruise. The gravitational attraction of the massive body allows this. Tracking data detect the gravitational field of a planet on approach a few days before encounter for a terrestrial planet and a few weeks in advance for the large outer planets.

For spacecraft that are in orbit about Mars or Venus, some orbital elements can be determined more accurately than others. It was estimated in 1976 that orbit shape and size can be determined to about 1 part per million, with spacecraft position along the orbit determined to comparable accuracy.[3] It was similarly estimated that the orientation angle of the orbit plane about any axis in the plane of the sky (the plane locally tangent to the celestial sphere) could be determined to 1 microradian. The orientation about the line of sight is much more difficult to determine[14,15,16] from Doppler tracking, with a typical accuracy as of 1976 being about 1 mrad.[3] Irregularities in a planet's gravity field limit the ability to accurately determine spacecraft orbits and particularly the ability to predict their future evolution.

EARLY EXPLORATION OF THE INNER SOLAR SYSTEM

During the 1960s the Ranger, Surveyor, and Lunar Orbiter series of robotic missions were launched, for the purposes of impacting the moon, landing softly on the moon, and photographing the moon from orbit, respectively. These series of robotic missions were designed to acquire critical knowledge and experience that would be needed in the piloted Apollo missions to follow. Beginning in 1959 several Pioneer missions were launched into heliocentric orbits to monitor the sun, measure properties of the interplanetary medium, and in one case to pass in the general vicinity of the moon. Some of this flight experience was to prove quite useful to NASA's early planetary missions. Our discussion here will begin with the first NASA missions to leave the Earth-moon system, for the purpose of flying to or near some planetary body.

Flyby Missions

The Mariner 2 spacecraft was launched on 27 August 1962 and passed by Venus at a radial distance of 34,773 km on 14 December 1962. A single midcourse maneuver was performed to compensate for launch orbit injection errors.[17,18] Communications in this mission were conducted at L-band (960 MHz), since this frequency band was already in use in the Ranger program.

Planetary encounter trajectories are often characterized using a B-plane representation, where the B-plane is centered on the planet and perpendicular to the spacecraft-planet relative velocity vector on approach, before the flight path has been affected by the planet's gravity.[19] Points in the B-plane represent where the spacecraft would pass the planet at closest approach, if the planet were massless. The Mariner 2 spacecraft missed its intended aimpoint in the B-plane by about 15,000 km, but this error was well within the acceptable range for this mission. The improvement in the estimate of the AU due to the Venus radar experiment of 1961 averted a much larger miss that would have negated much of the mission's scientific value.[1] In Mariner 2 and many future missions, the collection and processing of DSN tracking data, partially for navigational and partially for scientific purposes, yielded information that would be useful in navigating future missions. In this particular case, DSN tracking data were used to improve determinations of the masses of Venus and the moon and of the astronomical unit, as well as the ephemerides of Earth and Venus.

The Mariner 4 spacecraft was launched on 28 November 1964. One midcourse maneuver was performed in flight to Mars. The importance of accurately modeling solar radiation pressure effects on spacecraft motion was recognized – it was calculated in advance that solar radiation pressure would produce a cumulative outward displacement of the interplanetary flight path of about 19,000 km before arrival at Mars. The spacecraft passed within 9,846 km of the Martian surface on 14 July 1965. Pre-encounter orbit determination solutions had indicated that the distance at closest approach would be about 900 km less.[20,21,22] Uncertainty in the AU and small forces associated with the attitude control subsystem were thought to be the major contributors to this error. Subsequently, the spacecraft passed behind Mars as seen from Earth; and the radio signal ceased for 54 minutes before resuming. Twenty-two pictures were taken with the on-board television camera during the encounter and subsequently transmitted to Earth.

Communications at S-band at planetary distances had been recognized as superior to L-band communications and were technologically ready in time for the Mariner 4 mission.[1] Consequently, S-band communications were used in this mission and in those NASA planetary missions to follow for many years. Mariner 4 tracking data were used to obtain improved determinations of the masses of Mars and the moon and of the astronomical unit, improved ephemerides of Earth and Mars, and information about Martian atmospheric properties.

The Mariner 5 spacecraft was launched to Venus on 14 June 1967. After a single midcourse maneuver, the spacecraft passed about 4,000 km from Venus on 19 October 1967. Around the time of closest approach, the spacecraft passed behind Venus, as viewed from Earth. Spacecraft navigation accuracy was greatly improved relative to Mariner 2.[23] As with Mariner 2, DSN tracking data were used to obtain improved determinations of the masses of Venus and the moon and of the astronomical unit, as well as improved ephemerides of Earth and Venus. Information about atmospheric properties was obtained also. In this mission, ranging data were available for the first time at planetary distances.

The Mariner 6 spacecraft was launched on 24 February 1969. It flew past Mars on 31 July at a distance of 3431 km from the Martian surface. After closest approach, Mariner 6 passed behind Mars and reappeared after 25 minutes. The Mariner 7 spacecraft, a twin of Mariner 6, was launched on 27 March 1969. At closest approach on 5 August, Mariner 7 was 3430 km above the Martian surface. After closest approach, the spacecraft went behind Mars and emerged roughly 30 minutes later. The estimated spacecraft trajectories based on pre-encounter data turned out to be accurate to a few tens of km in the B-plane for Mariner 6.[24] Orbit determination results for Mariner 7 were a bit worse due to the apparent rupture of a battery case several days before encounter. This resulted in venting through openings in the thermal blanket, which imparted an unanticipated translational acceleration to the spacecraft.[25] DSN tracking data during both encounters were used to provide an accurate determination of the mass of Mars, the ephemerides of Mars and Earth, and the symmetry of the gravity field of Mars, as well as information about atmospheric properties.

Mariner 10 was the first spacecraft mission to use the gravitational attraction of one planet (Venus) to reach another (Mercury) and the first mission to visit two planets. The Mariner 10 spacecraft was launched on 3 November 1973. In addition to S-band uplink and downlink capabilities, the spacecraft included an experimental X-band downlink, coherent with the S-band uplink. A TCM was made 10 days after launch. Another corrective maneuver was made on 21 January 1974. The spacecraft passed Venus on

5 February 1974, at an altitude of 5768 km, within 17 km of the targeted aimpoint in the B-plane. This was the first NASA planetary mission to make extensive use of a sequential batch filter and smoother, as opposed to a conventional least-squares batch filter, for orbit determination.[26] Without sequential estimation, orbit determination errors would have been several times larger.

Due to an anomalous sequence of attitude control reaction jet firings prior to the Venus encounter, trajectory correction on the way to Mercury was executed by a single maneuver directed along the line from the spacecraft to the sun.[27] Such a directionally constrained maneuver eliminated the need to rotate the spacecraft and thereby minimized the chance of a recurrence of the anomalous jet firing behavior. The Mariner 10 spacecraft passed Mercury on 29 March 1974, at a distance of about 704 km from the surface. This first flyby of Mercury was used to modify the spacecraft's orbital energy such that two more flybys of Mercury were possible. After two more TCMs, unconstrained in direction as the prior anomalous jet firing behavior became better understood, a second encounter with Mercury occurred on 21 September 1974, at an altitude of 48,069 km. A third and last Mercury encounter at an altitude of 327 km occurred on 16 March 1975.

The ISEE-3 spacecraft, launched on 12 August 1978, was moved from its sun-Earth libration point orbit on 10 June 1982 and ultimately sent past Comet 21P/Giacobini-Zinner on 11 September 1985, after a sequence of lunar gravity-assist swingbys.[28]

In December of 1984, the Soviet Union launched the VEGA 1 and 2 spacecraft toward Venus and ultimately past Comet 1P/Halley. During the June 1985 flybys of Venus, DSN measurements consisting of one-way Doppler data and ΔDOR data (to be defined below) were used to determine the spacecraft flight paths, without the need to establish two-way links with spacecraft built and operated by a foreign space agency.[29]

Orbiting and Landing Missions

The Mariner 9 spacecraft was launched on 30 May 1971. A single TCM was performed en route to Mars,[30] with arrival occurring on 13 November 1971. A 15-minute rocket burn put the spacecraft into Mars orbit, making Mariner 9 the first spacecraft to orbit another planet. Through a couple of corrective orbit trim maneuvers, the periapsis was set to 1650 km and the orbital period to about 12 hours, so that synchronous data transmissions could be made to the Goldstone 64-m DSN antenna. It was found possible to predict the periapsis position of the spacecraft nine orbits in advance to an accuracy of 4 km.[31] The Mariner 9 mission provided information on the triaxial figure of Mars, the irregular gravity field, the Martian ephemeris, and atmospheric properties.[32] Mariner 9 was the first mission to make full use of the ODP software, predecessor software having been used in previous missions.

The Viking mission consisted of launches of two spacecraft to Mars, Viking 1, launched on 20 August 1975, and Viking 2, launched on 9 September 1975. Each spacecraft consisted of an orbiter and a lander. One TCM was needed for each spacecraft after departure from Earth and one was needed on approach to Mars. (Two TCMs were actually used on approach to Mars for the Viking 1 spacecraft, to resolve problems associated with a pressure regulator.) The Viking 1 and 2 spacecraft were delivered to the vicinity of Mars with B-plane accuracies of 25 km and 37 km, respectively.[33,34] Optical data, to be described below, were helpful in obtaining these accuracies.

The Viking 1 Orbiter was inserted into Mars orbit on 19 June 1976 and trimmed to a 1513 x 33,000 km, 24.7-hr site certification orbit on 21 June.[35] The Viking 2 Orbiter was inserted into Mars orbit on 7 August 1976 and trimmed to a 27.3-hr site certification orbit with a periapsis of 1509 km and an inclination of 55 degrees on 9 August. The orbit period was reduced to 24.6 hours by trim maneuvers on 25 August and 27 August. Following the approach used in the Mariner 9 mission, orbit determination was done by batch filtering a single orbit of Doppler data at a time, deleting data near periapsis.[36] Multi-revolution data fits were used to improve the model of the Martian gravity field.[37]

After one or more trim maneuvers in addition to those already mentioned, the Viking 1 Lander separated from its orbiter on 20 July 1976; and the Viking 2 Lander separated on 3 September 1976. At the time of separation, each lander was orbiting at about 4 km/s. After separation, rockets fired to begin lander deorbit. After a few hours at about 300-km altitude, the lander was reoriented for entry. An aeroshell with

an ablatable heat shield slowed the vehicle as it plunged through the atmosphere. At 5.8-km altitude and at a speed of about 250 m/s, the lander parachutes were deployed. Seven seconds later the aeroshell was jettisoned, and 8 seconds after that the three lander legs were extended. In 45 seconds the parachute slowed the lander to 60 m/s. At 1.5-km altitude, retro-rockets were ignited and fired until landing 40 seconds later at about 2.4 m/s. Navigational information during the descent was provided by gyros, accelerometers, a radar altimeter, and a terminal descent and landing radar.[38,39]

Orbital operations after the lander separations included orbit adjustments to change the rate at which the planetocentric longitude changed with each orbit, lower or raise the periapsis altitude, or change the orbit inclination. In addition, the Viking 1 Orbiter made close approaches to Phobos in February 1977.[40] The Viking 2 Orbiter made close approaches to Deimos in October 1977.

Orbiter-to-Earth communications in the Viking mission were done at S-band. An X-band orbiter downlink was also included for radio science and communications experiments. Lander-to-Earth communications were done at S-band. A UHF (381 MHz) antenna and relay radio provided a one-way link from the lander to the orbiter. The Viking mission provided the first flight demonstration of dual-frequency calibrations of charged particles in the interplanetary medium.[1]

The Pioneer Venus Orbiter (Pioneer 12) spacecraft was launched on 20 May 1978. Three TCMs were performed during interplanetary cruise to achieve the correct arrival time and aimpoint at Venus.[41] From insertion into a 24-hour orbit about Venus on 4 December 1978 to July 1980, periapsis was maintained between 142 and 253 km, with solar gravitational perturbations tending to raise the periapsis altitude. Thereafter, the periapsis was allowed to rise (to 2290 km at its maximum) and then fall, to conserve fuel. Single revolutions of Doppler data, with data near periapsis deleted, were processed for orbit determination.[42] Pioneer 12 determined the characteristics of the atmosphere and surface of Venus on a planetary scale and determined the planet's gravitational field harmonics from perturbations of the spacecraft orbit.

The Pioneer Venus Probe Bus (Pioneer 13) was launched on 8 August 1978. The bus carried four instrumented atmospheric entry probes to the vicinity of Venus and released them (on 15 to 20 November) for descent through the atmosphere to the planetary surface. Two small probes entered on the night side, and one small probe and the large probe entered on the day side of the planet on 9 December 1978. The bus portion of the spacecraft was targeted to enter the Venusian atmosphere at a shallow entry angle[43] and transmit data to Earth until the bus was destroyed by the heat of atmospheric friction during its descent. The probes stopped transmitting temperature data about 15 km above the surface of Venus, but two probes survived on the surface and transmitted other data for seconds to minutes.

The bus and the probes were spin stabilized. The spinning motion of the spacecraft made the interpretation of Doppler tracking data more complex than for three-axis stabilized planetary spacecraft. The circular polarization of the antenna, in combination with the rotation of the spacecraft, added a bias to the Doppler data. In addition, there was a sinusoidal ripple, due to the displacement of the antenna's center from the spin axis and the angular separation of the spin axis from the Earth line of sight. Prior to probe separation, orbits were determined almost entirely with two-way Doppler data, since the spacecraft was not compatible with conventional planetary ranging. However, ranging information could be derived by introducing frequency ramps in the Doppler data by means of a digitally controlled oscillator. The trajectories of the small probes were determined using one-way (downlink only) Doppler data, the accuracy of which was governed by the stability and bias characteristics of the on-board oscillators.[44]

DEEP SPACE NAVIGATION SYSTEM AUGMENTATIONS FOR OUTER SOLAR SYSTEM EXPLORATION

Differenced Two-Station Ranging

It has been noted above that Doppler-based orbit determination degrades in accuracy when the spacecraft declination is near zero. One means of circumventing this difficulty is to make use of ranging data between the spacecraft and two different tracking stations, at different latitudes. This concept is illustrated in Figure 7. If the baseline vector between two stations has a large north-south component, the

difference between the two station-spacecraft ranges will be strongly dependent on the spacecraft's declination. The planetary ranging system produced range measurements accurate to a few meters in the late 1970s, so that a two-station range difference involving stations in California and Australia, with a north-south baseline of about 7000 km, could provide a direct measurement of spacecraft declination to about 1 microrad. At moderate and high declinations, Doppler data could determine declination to 1/4 microrad, but the differenced range measurement provided a 1-microrad upper bound on errors at low declinations, avoiding a near-singular condition. Right ascension could usually be determined to 1/4 microrad for all geometries.

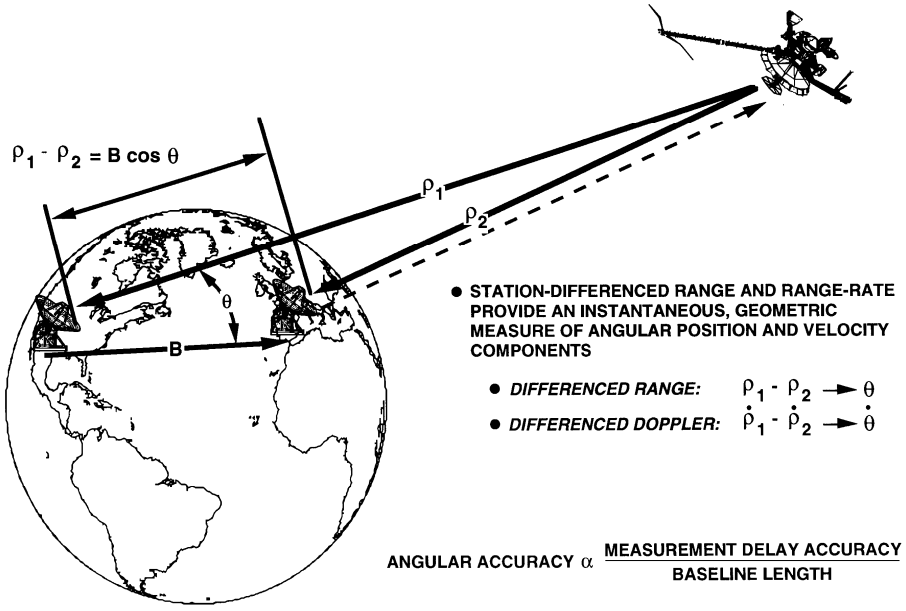

Figure 7 Angular Tracking Using Station-Differenced Observables

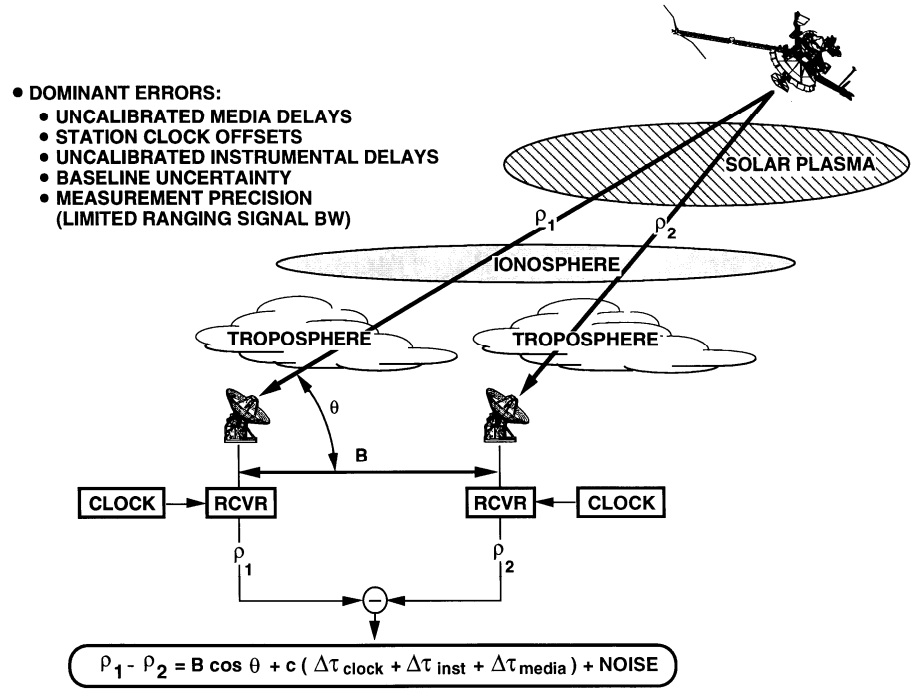

Figure 8 Differenced-Range Measurement Errors

Figure 8 indicates the major error sources associated with differenced-range measurements, which were developed as a navigational data type for use in the late 1970s.

Optical Navigation

In the last few months before an encounter with a distant natural body, a spacecraft's orbit accuracy can be improved with optical data. Optical measurements can be obtained from the science imaging instruments on board many planetary spacecraft. These optical instruments, designed to meet the stringent high-resolution and dynamic-range specifications required for scientific imaging of the planets and their natural satellites, have also proved to be excellent for optical navigation. Images of the target planets and their satellites against stellar backgrounds yield navigational information, as is shown in Figure 9. Optical data can be digitally encoded on board the spacecraft and transmitted to Earth using the same downlink signal from which radio navigation data are derived.

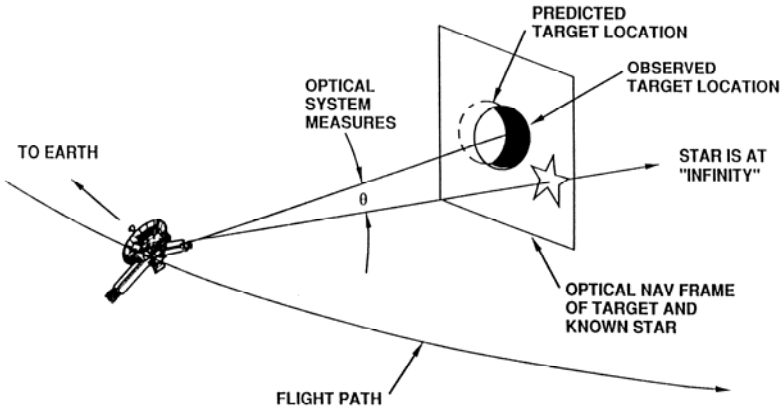

Figure 9 Navigation Measurements – Optical Data

In the early applications of optical navigation, optical data were processed in a man-machine interactive system, where full-frame images from the spacecraft were displayed on a videographics screen. There, an analyst could identify the target body and the background stars in an image. Limb-fitting algorithms were employed to locate the geometric center of the target body. The optical observables were then formed as the distances on the image plane between the target center and the identified stars. Dividing these distances by the camera focal length produced a measure of the angles between the target and the stars. Simulated observables and partial derivatives of the optical observations with respect to the spacecraft state and other parameters such as the target location and camera biases were then computed. An optical data file of the observable residuals and partial derivatives was produced, which was merged with the radio data files. Joint orbit estimates based on both radio and optical data could then be computed.

The navigational accuracies achievable with optical data are characterized differently than is the case with radio metric data. The optical observation is target-relative rather than Earth-based, a considerable advantage since the effects of the target-relative ephemeris errors are minimized, and the spacecraft is much closer to the target than to the Earth when the final flight-path corrections are performed. Since the optical observable measures angles directly, the strength of the measurement is relatively insensitive to geometry, unlike Doppler data. A limiting error is the resolution of the camera. Line and pixel (picture element) spacings in the Voyager vidicon imaging system were about 0.015 mm, and the optical focal length was 1.5 m. Therefore, half-pixel resolution produced an angular resolution of 5 microrad. The ultimate positional accuracy obtainable with optical data is limited by the ability to determine the gravitational center of the target body from the limb and terminator measurements in the optical images. The centerfinding capability was found to be better than 1% of target-body radius for regularly shaped objects, in early applications of optical navigation.

Angular data accurate to 5 microrad provide orbits good to about 1 km for every 200,000 km of distance from the target body. For approach speeds of around 10 km/s, optical data are useful for improving radio-determined orbits over the final month or so before a planetary encounter.

Very Long Baseline Interferometry

Figure 10 shows two widely separated antennas receiving broadband radio signals from the same distant radio source. By correlating the signals received at the two stations, the difference in arrival times can be calculated, which yields information about the angle between the direction to the source and the baseline vector between the stations. (The measured time delay consists of the actual geometric delay plus delays due to station clock offsets and differences in signal delays through the ionosphere, troposphere, instrumentation, etc.[10]) The use of widely separated antennas to study distant radio sources is called very long baseline interferometry (VLBI). It has numerous scientific applications and several navigational applications as well.

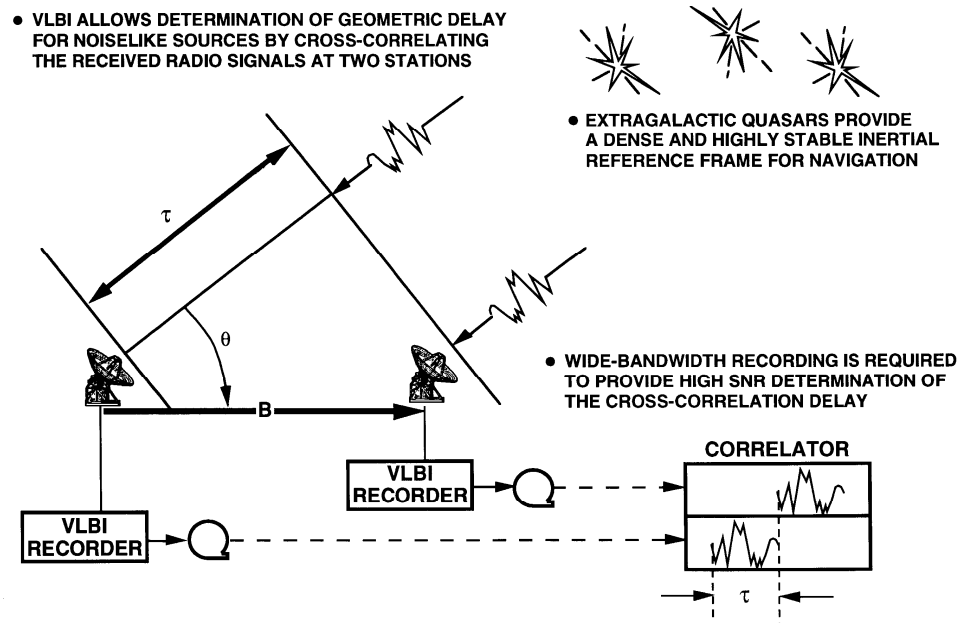

Figure 10 Very Long Baseline Interferometry

One navigational application is that with sufficient measurements involving a large number of extragalactic natural radio sources (or quasars) and multiple ground antennas, it is possible to determine the positions of the various sources on the celestial sphere, as well as the positions of the various antennas on the Earth's surface. Indeed, this technique offered a means of substantially improving both the knowledge of DSN crust-fixed station locations and the modeling of the Earth's rotation and polar motion when it was put into use in connection with the antennas of the DSN. It also provided an improved means to measure time offsets between DSN complexes and the drift rates of station clocks.[2]

A second navigational application of VLBI involves the differencing of VLBI observations of a spacecraft and an angularly nearby quasar with a well known position, as is shown in Figure 11.[45] The explicit differencing removes or substantially reduces the effects of common errors. Station clock offsets and instrumental group delays can be almost entirely cancelled. Errors due to uncalibrated media effects and poorly modeled baseline vectors can be greatly reduced. The extent to which errors are eliminated in the differencing process depends on how angularly close the spacecraft and quasar are, the time offset between observations (since the two objects are typically observed in an alternating sequence, not simultaneously), and the degree of similarity in the spectral characteristics of the signals.[10]

Quasars have broadband signals with nearly flat spectra over many gigahertz. Spacecraft signals are band limited and may contain tones that are added for VLBI tracking. Multiple tones are used to resolve

ambiguities in spacecraft delay. (The widest tone spacing is 38 MHz at X-band.) The delay determined from spacecraft measurements is called differential one-way range (DOR). The differential delay between a spacecraft and a quasar is called ΔDOR. The ΔDOR measurement accuracy figure of 30 nanorad shown in Figure 11 was as of 1992.

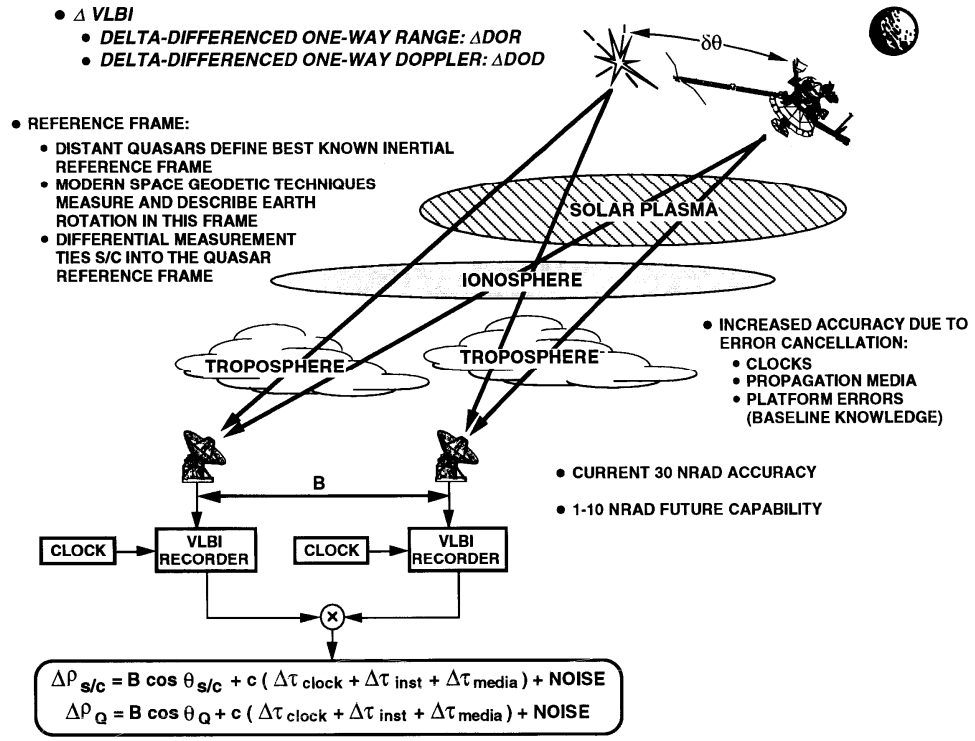

Figure 11 Spacecraft-Quasar Differential Angular Techniques

If the ambiguities in spacecraft delay are not resolved, useful information is still available regarding the delay rate. This can be used to improve orbit determination accuracy for planetary orbiters by providing information about spacecraft velocity perpendicular to the line of sight, resolving the difficulty that Doppler data have in determining orbit rotations about this line.[46]

The effective use of ΔDOR data requires that the planetary ephemerides be known accurately in the radio reference frame defined by the quasar locations. Planetary ephemerides were developed over many years in a different, self-consistent reference frame. Before VLBI observations were made of spacecraft during planetary encounters, there was a misalignment of several hundred nanoradians between the two frames. It is estimated that the radio/planetary frame-tie error had been reduced to 25 nrad by 1992.[10]

EARLY EXPLORATION OF THE OUTER SOLAR SYSTEM

Pioneers 10 and 11

The Pioneer 10 spacecraft, launched on 3 March 1972, was the first to be sent to the outer solar system and the first to investigate Jupiter. The spacecraft achieved its closest approach to Jupiter on 3 December 1973, at a periapsis radius of about 200,000 km.[47]

The Pioneer 11 spacecraft, launched 6 April 1973, was the second to investigate Jupiter and the outer solar system. During its closest approach to Jupiter, on 4 December 1974, the spacecraft passed within 34,000 km of the cloud tops. It traveled through Jupiter's gravitational field in such a way as to be redirected toward Saturn. It passed by Saturn on 1 September 1979, at a distance of 21,000 km from Saturn's cloud tops.[48] The Pioneer 10 and 11 spacecraft were spin stabilized.

Voyager Encounters with Jupiter and Saturn

The Voyager 1 and 2 spacecraft were launched on 5 September and 20 August 1977, respectively. The Voyager 1 spacecraft arrived at Jupiter on 5 March 1979 and passed within 350,000 km of the planet, while being targeted to a close (20,000-km) flyby of the satellite Io.[49] The Voyager 2 spacecraft flew by Jupiter on 9 July 1979, passing within 730,000 km of the planet and encountering the satellite Ganymede at a distance of 62,000 km. (The distances stated here are measured from the centers of the various bodies.)

With a dual-frequency (S- and X-band) downlink capability, the Voyager spacecraft were the first to utilize X-band as the primary telemetry link frequency. For the Voyager encounters with Jupiter, radio metric data alone permitted sufficiently accurate navigation to fulfill the scientific objectives of the encounters. Optical data were used also and enhanced the navigational accuracy. For the Saturn encounters to follow, however, radio metric data alone could not provide sufficiently accurate navigation to fulfill the scientific objectives; and optical data were relied upon for the first time to meet mission objectives, rather than to enhance accuracy.

The Voyager 1 spacecraft flew by Saturn on 12 November 1980. The flight path was targeted so as to pass within 7000 km of Titan, 18 hours before closest approach to Saturn. TCMs were performed 33 days and 5 days before encounter to achieve the desired targeting. After the close encounter with Titan, the flight path passed directly behind the satellite, as viewed from the Earth, such that the passage of the radio signal through the atmosphere of Titan could provide data on atmospheric properties. The spacecraft then passed by (185,000 km), and then behind, Saturn and its rings, resulting in similar radio occultations.[50]

The Voyager 1 spacecraft was required to perform a diametric Earth occultation with Titan to within a tolerance of 265 km and then, after closest approach to Saturn, to pass through a presumed 5000-km wide gap in Saturn's E-ring. Uncertainties in the dispersed flight path after the Titan and Saturn flybys created a navigational challenge for controlling the instrument pointing for observations of the Saturnian satellites on the outbound leg of the Saturnian system encounter. During the Titan encounter, Doppler data were quickly processed to determine the flyby trajectory to high precision. This led to accurate instrument-pointing adjustments for the outbound imaging of the satellites Mimas, Enceladus, Dione, and Rhea. The delivery to Titan was accurate to 330 km, with the error only 37 km in the most important direction, allowing a nearly perfect diametrical occultation by Titan to be achieved. The flight path was also sufficiently accurate that the spacecraft passed safely through the E-ring gap on its escape from the Saturnian system.

Special-purpose satellite ephemeris propagation software for the Galilean and Saturnian satellite systems was developed in advance of the encounters; and an extensive pre-encounter ephemeris generation activity, including the acquisition of many new astrometric plate observations, was undertaken. The satellite ephemerides were updated as the spacecraft orbits on approach were determined from the optical navigation measurements. The analytical theory-based Saturn satellite ephemeris propagator, used for the preflight ephemeris generation, was not accurate enough for the reduction of optical measurements of Titan. Therefore, the preflight Titan ephemeris theory parameters had to be transformed to a Cartesian state vector, and the subsequent path of Titan numerically integrated.[51] Many spacecraft orbit solutions were processed and reviewed during the approach to Titan before a final, successful one was chosen.

The primary concern in the navigation of the Voyager 2 spacecraft to Jupiter and Saturn was the retention of adequate propellant to reach Uranus. During a planetary swingby, an error in either the approach trajectory or the mass of the planet leads to an error in the outbound direction of travel, which must be corrected with a propulsive maneuver. This maneuver reduces the remaining propellant available for both attitude control and subsequent flight path corrections.

The Voyager 2 spacecraft encountered the Saturnian system on 25 August 1981. The spacecraft passed by Saturn at a distance of 161,000 km and then passed within 100,000 km of the satellites Enceladus and Tethys. The Voyager 2 navigation requirements at Saturn were neither as stringent nor as complex as those of Voyager 1. The incoming trajectory was controlled quite accurately, resulting in small corrective maneuvers after the encounter and leaving ample propellant for future use.

Optical navigation was required for the first time in the Voyager mission to meet a deep space mission's objectives. It had been demonstrated previously in several Mariner missions[52,53,54,55] and the Viking mission[34] and had improved the orbit determination accuracy, but it had not been essential to mission success. Optical measurements were employed over the final few months before each Voyager encounter and served as the most accurate navigational measurements for the planetary encounters. Doppler-based orbit determination served as an initialization and backup to optical navigation during the Jupiter approaches. The Doppler system, augmented with differenced two-station range measurements, was adopted as a backup at Saturn.[56] (The Voyager 1 encounter with Saturn occurred near zero declination, motivating the development of the differenced two-station ranging technique.)

Optical navigation was performed in the Voyager mission using images of the satellites of Jupiter and Saturn, not the planets themselves. The smaller sizes of the satellites and their more clearly defined surfaces made them much more attractive as optical navigation targets than the central planets. In addition, many of the encounter target conditions were relative to the satellites themselves, so that knowledge of the path of the target satellite was required to the same accuracy as the spacecraft flight path.

The differenced two-station range measurement capability, although a wise investment in overall mission reliability, did not make a critical contribution to orbit determination accuracy, because of the performance of the optical navigation process. Moreover, it was shortly superseded by the ΔDOR technique, with similar information content but substantially improved accuracy.

Voyager-2 Encounters with Uranus and Neptune

During the outward travels of the Voyager spacecraft, a number of upgrades were made to the DSN. These included the replacement of the deep space 26-m antennas with 34-m antennas during the late 1970s and early 1980s, as well as the conversion of the three 64-m antennas to 70-m antennas, which became available for operational use in 1987-1988.

The navigational challenges in the Uranus and Neptune encounters of the Voyager 2 spacecraft were similar in many respects to those in the Jupiter and Saturn encounters, but certain new problems arose in addition. Due to the greater geocentric distances of Uranus and Neptune, ephemeris uncertainties for these bodies and their natural satellites, based on telescopic observations from Earth, were significantly larger than for Jupiter and Saturn. Pre-encounter ephemeris errors for Uranus, Neptune, and Triton (relative to Neptune) were about 5000, 10,000, and 6700 km, respectively. Corresponding a priori ephemeris errors for Jupiter and Saturn had been only 400 and 800 km. An effort was undertaken for several years to improve the ephemerides of Uranus, Neptune, and their satellites by expanding the observational data base and using suitable dynamical modeling techniques.[57,58] Even with some improvement in these Earth-based ephemerides, however, on-board optical data were extremely important for accurate prediction and control of the spacecraft's trajectory relative to these planets and their satellites.

On-board optical data are quite effective in determining the position components of a spacecraft that are perpendicular to its nominal flight path in a target-body centered reference frame, but they yield relatively little information about the position along the flight path until quite close to encounter. Radio metric data can be helpful in estimating these time-of-flight errors by sensing the gravitational field of the target planet. Time-of-flight errors tended to remain quite large in the approaches to Uranus and Neptune, however, for several reasons: 1) the masses of Uranus and Neptune are smaller than those of Jupiter and Saturn, and the approach speeds were higher in the encounters with the former, so that the gravitational fields of Uranus and Neptune did not exert a significant influence on the trajectory until relatively close to encounter; 2) the encounters occurred at sufficiently large negative geocentric declinations that relatively little tracking data could be gathered at the two DSN tracking complexes in the northern hemisphere; and 3) the very long round-trip light times of 5-1/2 hr at Uranus and 8-1/4 hr at Neptune substantially reduced the amount of two-way, coherent tracking data that could be collected.

The use of ΔDOR data offered a means of reducing the impacts of these adverse factors. Only short periods of overlapping station coverage were needed for accurate geocentric angle determination using ΔDOR techniques. Thus, limited tracking coverage at the northern hemispheric stations was not a serious problem. Moreover, ΔDOR is a one-way data type, so that the round-trip light time is not particularly

important. The utilization of the full potential of ΔDOR data for orbit determination requires a wide-band spacecraft transponder. The Voyager transponder was not designed in this way. However, the 360-kHz square-wave telemetry subcarrier used to modulate the S- and X-band downlink carriers could be used to generate a signal of adequate bandwidth. Observation of the fifth harmonics of the telemetry subcarrier, centered about the downlink carrier frequency, produced a spanned bandwidth of 3.6 MHz, for example. Due to bandwidth limitations, the ΔDOR data obtained in this manner were not accurate to the 30-nrad performance level mentioned earlier. However, the data were still quite useful in both encounter and cruise phases.

The nominal encounter geometry was such that both geocentric and heliocentric occultations of the spacecraft by Uranus were virtually guaranteed. The closest satellite encounter was with Miranda, at a distance of less than 30,000 km. Since the uncertainty in time of flight did not diminish appreciably until relatively close to encounter, errors in arrival time would have been relatively expensive to correct, in terms of propellant consumption, once they were finally known. As a consequence, the final TCM was used to control the position perpendicular to the direction of relative motion, but not time of flight. The controlling of two, rather than three, encounter parameters resulted in a considerable propellant savings but necessitated a late adjustment in the timing of data-collection sequences. Accurate approach navigation allowed a mosaic of high-resolution images of Miranda to be obtained.[59,60,61]

The nominal flyby geometry at Neptune was subject to fewer constraints than at Uranus, there being no subsequent planet to encounter, leaving more options available for encounter geometry. Geocentric and heliocentric occultations of the spacecraft by Neptune could be easily achieved. Similar occultations by Neptune's satellite Triton were also strongly desired, but presented a much greater navigational challenge due to the much smaller size of Triton.

Concerns for spacecraft safety led to requirements that the vehicle pass no closer than 28,680 km from the center of Neptune at the time of closest approach (to avoid the outermost portions of Neptune's atmosphere) and no closer than 73,500 km from the center when crossing Neptune's equatorial plane (to avoid collisions with ring particles). Refinement of the estimates of the mass of Neptune, the orientation of its spin axis, and the ephemeris of Triton as the encounter became closer necessitated some late changes in the planned encounter trajectory.

The achievement of occultations of both the sun and the Earth by Triton was more difficult than achieving either occultation alone. In addition, estimates of the radius of Triton were revised downward in steps from well over 2000 km to 1360 km, as the encounter became closer, increasing the flight path accuracy required to achieve the dual occultation. Accurate prediction of the flight path was also required during the passage through the Neptunian system in order to point the cameras accurately at Triton and other natural satellites (some of which were discovered as the encounter unfolded) and in order to point the spacecraft antenna properly during the occultation of the Earth by Neptune.

All of these requirements on navigational accuracy were met.[62,63,64,65] The time of arrival at Neptune was controlled well enough (260 s) by the first of three planned approach TCMs that the second scheduled maneuver could be omitted, eliminating a subsequent two-day outage of two-way Doppler data, due to extreme temperature sensitivity on the part of the partially failed spacecraft receiver. The third scheduled TCM was made with attitude control thrusters, which avoided the heating problem and provided the final correction needed to achieve the dual occultations by Triton.

The safety requirements were met by delivering the spacecraft to a Neptune closest approach radius of 29,240 km, just 90 km outside the nominal distance. Around the time of closest approach to Neptune, the spacecraft position was predicted to an accuracy of 40 km and the time of arrival to 0.6 s. The distance at the time of ring-plane crossing was 85,300 km. The desired aimpoint in the Triton dual occultation zone was achieved to within 220 km, a small error given that the Triton encounter occurred about 5 hr after the close passage over Neptune's polar regions, with errors on approach to Neptune tending to be substantially magnified by the gravitational bending of the flight path. Late updates to instrument and antenna pointing sequences were made based on the most current orbit determination solutions.

CONCLUSIONS

The exploration of the solar system using robotic vehicles began in the early 1960s with the Mariner 2 mission to Venus. Over the years that followed, leading up to the 1989 Voyager encounter with Neptune, planetary mission objectives became increasingly sophisticated, as the early single-planet flybys gave way to planetary orbiters, multi-planet flybys, and planetary landers. During this time the navigational capabilities employed in these missions increased greatly in accuracy, as required by the scientific objectives of the missions and as enabled by improvements in technology.

Radio metric data derived from the spacecraft-to-ground communication link were used throughout this time to yield information about spacecraft position and velocity and other parameters of interest, with Doppler, ranging, and ΔDOR data types developed in sequence. The evolution of communication frequencies from L-band, to S-band, to X-band, and extensive measurement and dynamical model development allowed substantial improvements in navigational accuracy. Optical data, derived from on-board imaging systems, were tested and put into operational use during the 1970s and 1980s, enabling further improvements in target-relative navigational accuracies. Computing capabilities and techniques improved substantially during the 1960s, 1970s, and 1980s, allowing problems of greater sophistication to be addressed.

ACKNOWLEDGMENT

The research described in this paper was carried out at the Jet Propulsion Laboratory, California Institute of Technology, under a contract with the National Aeronautics and Space Administration.

REFERENCES

1. D. J. Mudgway, *Uplink-Downlink: A History of the Deep Space Network 1957-1997*, NASA SP-2001-4227, 2001.
2. N. A. Renzetti, et al., *The Deep Space Network – An Instrument for Radio Navigation of Deep Space Probes*, Jet Propulsion Laboratory Publication 82-102, Pasadena, CA, Dec. 15, 1982.
3. W. G. Melbourne, "Navigation Between the Planets," *Scientific American*, Vol. 234, June 1976, pp. 58-74.
4. T. D. Moyer, *Mathematical Formulation of the Double-Precision Orbit Determination Program (DPODP)*, Technical Report 32-1527, Jet Propulsion Laboratory, Pasadena, CA, May 15, 1971.
5. T. D. Moyer, *Formulation for Observed and Computed Values of Deep Space Network Data Types for Navigation*, John Wiley and Sons, Inc., Hoboken, NJ, 2003.
6. J. E. Ekelund, "The JPL Orbit Determination Software System," in *Advances in the Astronautical Sciences: Astrodynamics 1979*, Vol. 40, Part I, ed. P. Penzo, et al., Univelt, San Diego, 1980, pp. 79-88.
7. M. R. Warner, M. W. Nead, and R. H. Hudson, *The Orbit Determination Program of the Jet Propulsion Laboratory*, Technical Memorandum 33-168, Jet Propulsion Laboratory, Pasadena, CA, Mar. 18, 1964.
8. M. R. Warner and M. W. Nead, *SPODP – Single Precision Orbit Determination Program*, Technical Memorandum 33-204, Jet Propulsion Laboratory, Pasadena, CA, Feb. 15, 1965.
9. J. Ellis, "Large Scale State Estimation Algorithms for DSN Tracking Station Location Determination," *The Journal of the Astronautical Sciences*, Vol. XXVIII, Jan.-Mar. 1980, pp. 15-30.
10. C. L. Thornton and J. S. Border, *Radiometric Tracking Techniques for Deep-Space Navigation*, John Wiley and Sons, Inc., Hoboken, NJ, 2003.
11. J. F. Jordan and L. J. Wood, "Navigation, Space Mission," *Encyclopedia of Physical Science and Technology*, Vol. 8, Academic Press, 1987, pp. 744-767.
12. T. W. Hamilton and W. G. Melbourne, "Information Content of a Single Pass of Doppler Data from a Distant Spacecraft," in *The Deep Space Network, Space Programs Summary 37-39*, Vol. III, Jet Propulsion Laboratory, Pasadena, CA, May 31, 1966, pp. 18-23.

13. C. R. Gates, *A Simplified Model of Midcourse Maneuver Execution Errors*, Technical Report 32-504, Jet Propulsion Laboratory, Pasadena, CA, Oct. 15, 1963.
14. R. K. Russell, "Influence of Orbital Parameters on Satellite Orbit Determination Accuracy," in *The Deep Space Network, Space Programs Summary 37-61*, Vol. II, Jet Propulsion Laboratory, Pasadena, CA, Jan. 31, 1970, pp. 32-38.
15. L. J. Wood, "Orbit Determination Singularities in the Doppler Tracking of a Planetary Orbiter," *Journal of Guidance, Control, and Dynamics*, Vol. 9, July-Aug. 1986, pp. 485-494.
16. R. K. Russell and S. W. Thurman, "An Analytic Development of Orbit Determination for a Distant Planetary Orbiter," AAS Paper 89-402, AAS/AIAA Astrodynamics Conference, Stowe, VT, Aug. 1989.
17. F. L. Barnes, et al., "Mariner 2 Flight to Venus," *Astronautics*, Vol. 7, Dec. 1962, pp. 66-72.
18. J. N. James, "The Voyage of Mariner II," *Scientific American*, July 1963, pp. 70-84.
19. W. Kizner, *A Method of Describing Miss Distances for Lunar and Interplanetary Trajectories*, External Publication 674, Jet Propulsion Laboratory, Pasadena, CA, Aug. 1, 1959.
20. J. N. James, "The Voyage of Mariner IV," *Scientific American*, Vol. 214, Mar. 1966, p. 42.
21. D. A. Tito, "Trajectory Design for the Mariner-Mars 1964 Mission," *Journal of Spacecraft and Rockets*, Vol. 4, Mar. 1967, pp. 289-296.
22. G. W. Null, H. J. Gordon, and D. A. Tito, *The Mariner IV Flight Path and Its Determination from Tracking Data*, Technical Report 32-1108, Jet Propulsion Laboratory, Pasadena, CA, Aug. 1, 1967.
23. G. Pease, et al., *The Mariner V Flight Path and Its Determination from Tracking Data*, Technical Report 32-1363, Jet Propulsion Laboratory, Pasadena, CA, July 1, 1969.
24. H. J. Gordon, et al., *The Mariner VI and VII Flight Paths and Their Determination from Tracking Data*, Technical Memorandum 33-469, Jet Propulsion Laboratory, Pasadena, Calif., Dec. 1, 1970.
25. H. J. Gordon, S. K. Wong, and V. J. Ondrasik, "Analysis of Mariner VII Pre-Encounter Anomaly," *Journal of Spacecraft and Rockets*, Vol. 8, Sept. 1971, pp. 931-937.
26. C. S. Christensen and S. J. Reinbold, "Navigation of the Mariner 10 Spacecraft to Venus and Mercury," *Journal of Spacecraft and Rockets*, Vol. 12, May 1975, pp. 280-286.
27. M. H. Bantell and J. B. Jones, "Navigation Results of the Mariner Venus/Mercury 1973 Mission," Paper 75-84, AIAA 13th Aerospace Sciences Meeting, Pasadena, Calif., Jan. 1975.
28. L. Efron, R. J. Muellerschoen, and R. I. Premkumar, "Navigating the International Cometary Explorer for Encounter with Comet Giacobini-Zinner," *Proceedings of the 15th International Symposium on Space Technology and Science*, Vol. 2, Tokyo, Japan, 1986, pp. 1751-1762.
29. R. S. Bhat, J. Ellis, and T. P. McElrath, "Navigation with Noncoherent Data: A Demonstration for VEGA Venus Flyby Phase," *Proceedings of the AIAA/AAS Astrodynamics Conference*, Minneapolis, MN, Aug. 1988, pp. 344-350.
30. R. T. Mitchell and W. J. O'Neil, "Maneuver Design and Implementation for the Mariner 9 Mission," *Journal of Spacecraft and Rockets*, Vol. 10, Nov. 1973, pp. 723-730.
31. G. H. Born, et al., "The Determination of the Satellite Orbit of Mariner 9," *Celestial Mechanics*, Vol. 9, May 1974, pp. 395-414.
32. W. J. O'Neil, et al., *Mariner 9 Navigation*, Technical Report 32-1586, Jet Propulsion Laboratory, Pasadena, CA, Nov. 13, 1973.
33. K. H. Rourke, et al., "The Determination of the Interplanetary Orbits of Vikings 1 and 2," Paper 77-71, AIAA 15th Aerospace Sciences Meeting, Los Angeles, Calif., Jan. 1977.
34. W. J. O'Neil, et al., *Viking Navigation*, Jet Propulsion Laboratory Publication 78-38, Pasadena, CA, Nov. 15, 1979.
35. G. R. Hintz, D. L. Farless, and M. J. Adams, "Viking Orbit Trim Maneuvers," Paper 78-1394, AIAA/AAS Astrodynamics Conference, Palo Alto, CA, Aug. 1978.

36. C. E. Hildebrand, et al., "Viking Satellite Orbit Determination," Paper 77-70, AIAA 15th Aerospace Sciences Meeting, Los Angeles, Calif., Jan. 1977.
37. E. J. Christensen and B. G. Williams, "Mars Gravity Field Derived from Viking-1 and Viking-2: The Navigation Result," *Journal of Guidance and Control*, Vol. 2, May-June 1979, pp. 179-183.
38. R. N. Ingoldby, "Guidance and Control System Design of the Viking Planetary Lander," *Journal of Guidance and Control*, Vol. 1, May-June 1978, pp. 189-196.
39. E. A. Euler, G. L. Adams, and F. W. Hopper, "Design and Reconstruction of the Viking Lander Descent Trajectories," *Journal of Guidance and Control*, Vol. 1, Sept.-Oct. 1978, pp. 372-378.
40. R. E. Diehl, M. J. Adams, and E. A. Rinderle, Jr., "Phobos Encounter Trajectory and Maneuver Design," *Journal of Guidance and Control*, Vol. 2, Mar.-Apr. 1979, pp. 123-129.
41. G. R. Hintz, "An Interplanetary Targeting and Orbit Insertion Maneuver Design Technique," *Journal of Guidance, Control, and Dynamics*, Vol. 5, Mar.-Apr. 1982, pp. 210-217.
42. R. A. Jacobson, et al., "Orbit Determination Strategy and Results for the Pioneer Venus Orbiter Mission," *Advances in the Astronautical Sciences: Astrodynamics 1979*, Vol. 40, ed. P. Penzo, et al., Univelt, San Diego, 1980, pp. 251-271.
43. W. F. Brady, "Pioneer Venus Probe Targeting Maneuver Design," *Advances in the Astronautical Sciences: Astrodynamics 1979*, Vol. 40, Part I, ed. P. Penzo, et al., Univelt, San Diego, 1980, pp. 233-250.
44. S. K. Wong and H. M. Guerrero, "The Strategy and Technique in Determining the Orbits of the Pioneer Venus Multiprobe Bus and Probes," AAS Paper 79-181, AAS/AIAA Astrodynamics Conference, Provincetown, MA, June 1979.
45. W. G. Melbourne and D. W. Curkendall, "Radio Metric Direction Finding: A New Approach to Deep Space Navigation," AAS/AIAA Astrodynamics Conference, Jackson, WY, Sept. 1977.
46. P. B. Esposito, et al., "Narrowband Differential Interferometry Applied to Pioneer Venus Orbiter," AAS Paper 83-310, AAS/AIAA Astrodynamics Conference, Lake Placid, NY, Aug. 1983.
47. S. K. Wong and A. J. Lubeley, "Orbit Determination Strategy and Results for the Pioneer 10 Jupiter Mission," AIAA Mechanics and Control of Flight Conference, Anaheim, CA, Aug. 1974.
48. R. B. Frauenholz and W. F. Brady, "Maneuver Sequence Design for the Post-Jupiter Leg of the Pioneer Saturn Mission," *Journal of Spacecraft and Rockets*, Vol. 14, July 1977, pp. 395-400.
49. J. K. Campbell, S. P. Synnott, and G. J. Bierman, "Voyager Orbit Determination at Jupiter," *IEEE Transactions on Automatic Control*, Vol. AC-28, March 1983, pp. 256-268.
50. J. K. Campbell, et al., "Voyager I and Voyager II Saturn Encounter Orbit Determination," Paper 82-0419, AIAA 20th Aerospace Sciences Meeting, Orlando, FL, Jan. 1982.
51. R. A. Jacobson, J. K. Campbell, and S. P. Synnott, "Satellite Ephemerides for Voyager Saturn Encounter," AIAA Paper 82-1472, AIAA/AAS Astrodynamics Conference, San Diego, CA, August 1982.
52. T. C. Duxbury, "Navigation Data from Mariner Mars 1969 TV Pictures," *Navigation*, Vol. 17, Fall 1970, pp. 219-225.
53. T. C. Duxbury, G. H. Born, and N. Jerath, "Viewing Phobos and Deimos for Navigating Mariner 9," *Journal of Spacecraft and Rockets*, Vol. 11, April 1974, pp. 215-222.
54. N. Jerath and H. Ohtakay, "Mariner IX Optical Navigation Using Mars Limb Data," *Journal of Spacecraft and Rockets*, Vol. 11, July 1974, pp. 505-511.
55. C. H. Acton and H. Ohtakay, "Mariner-Venus-Mercury Optical Navigation Demonstration: Results and Implications for Future Missions," AAS Paper 75-088, AAS/AIAA Astrodynamics Conference, Nassau, Bahamas, July 1975.
56. T. H. Taylor, et al., "Performance of Differenced Range Data Types in Voyager Navigation," *Journal of Guidance, Control, and Dynamics*, Vol. 7, May-June 1984, pp. 301-306.

57. R. A. Jacobson and E. M. Standish, “Satellite Ephemerides for the Voyager Uranus Encounter,” AIAA Paper 84-2024, AIAA/AAS Astrodynamics Conf., Seattle, WA, Aug. 1984.
58. R. A. Jacobson, “Satellite Ephemerides for the Voyager Neptune Encounter,” *Advances in the Astronautical Sciences: Astrodynamics 1987*, Vol. 65, Pt. I, ed. J. Soldner, et al., Univelt, San Diego, 1988, pp. 657-680.
59. D. L. Gray, et al., “Voyager 2 Uranus Navigation Results,” *Proceedings of the AIAA/AAS Astrodynamics Conference*, Williamsburg, VA, Aug. 1986, pp. 144-151.
60. T. H. Taylor, et al., “Orbit Determination for the Voyager II Uranus Encounter,” *Proceedings of the AIAA/AAS Astrodynamics Conference*, Williamsburg, VA, Aug. 1986, pp. 178-191.
61. S. P. Synnott, et al., “Interplanetary Optical Navigation: Voyager Uranus Encounter,” *Proceedings of the AIAA/AAS Astrodynamics Conference*, Williamsburg, VA, Aug. 1986, pp. 192-206.
62. D. L. Gray, et al., “Voyager 2 Neptune Navigation Results,” *Proceedings of the AIAA/AAS Astrodynamics Conference*, Portland, OR, Aug. 1990, pp. 108-117.
63. G. D. Lewis, et al., “Voyager 2 Orbit Determination at Neptune,” *The Journal of the Astronautical Sciences*, Vol. 40, July-Sept. 1992, pp. 369-406.
64. D. C. Roth, et al., “Performance of Three-Way Data Types during Voyager's Encounter with Neptune,” *Proceedings of the AIAA/AAS Astrodynamics Conference*, Portland, OR, Aug. 1990, pp. 129-134.
65. J. E. Riedel, et al., “Optical Navigation during the Voyager Neptune Encounter,” *Proceedings of the AIAA/AAS Astrodynamics Conference*, Portland, OR, Aug. 1990, pp. 118-128.